^1H and ^{13}C NMR Studies on the Conformation of *N*-Methyl Diastereomers of (+)-Glaucine Hydrotrifluoroacetate, an Aporphine Alkaloid Salt

Robert Glaser *[a] **and Michael A. Bernstein** *[b]
[a] *Department of Chemistry, Ben Gurion University of the Negev, Beersheva 84105, Israel*
[b] *Department of Medicinal Chemistry, Merck Frosst Centre for Therapeutic Research, PO Box 1005, Pointe Claire-Dorval, Québec, Canada H9R 4P8*

A 3:1 ratio of *N*-methyl diastereomers of (+)-glaucine hydrotrifluoroacetate was observed at slow exchange by ^1H NMR spectroscopy (300 MHz, CD_2Cl_2), but the spectrum was too complex to be interpreted solely by one-dimensional methods. However, the E.COSY 2D NMR spectrum afforded all proton chemical shift and coupling constant data for both *N*-methyl diastereomers. Surprisingly, there are few or no cases where the E.COSY data have been analysed manually and have thereby effected a full assignment of the ^1H NMR spectrum of a molecule. While X-ray crystallographically determined structures of aporphine alkaloids have B-rings with either *M*- or *P*-conformations [as denoted by the sign of the C(3a)–C(4)–C(5)–N torsion angle], measured vicinal coupling constants together with difference-NOE experiments showed both solution-state species of (+)-glaucine to have the *M*-conformation for the B-ring. The major and minor solution-state species differ by configuration at nitrogen: the 6*S*,6a*S*-major species has an equatorial *N*-methyl group, and the 6*R*,6a*S*-minor species has an axial one. The major contributor to the fast exchange limit structure of glaucine free base has an equatorial *N*-methyl group.

The evolution of 2D NMR has been one where the intense period of pulse program discovery of the late 1970s has given way to a time, now, when these experiments are being widely applied. To this end, some attention has been focussed on ways in which experiments may be combined to give procedures for effecting spectral assignment.[1] The ^1H 2D correlation spectroscopy (COSY) experiment has seen wide application as a method for determining which multiplets share a scalar coupling. Of the phase-sensitive 2D COSY-like experiments, E.COSY[2] [Exclusive COSY] is advantageous in that it simplifies the cross-peak pattern to the point where it can be relatively easily analysed, and ambiguities resulting from overlap are minimized. The signs and magnitudes of coupling constants can be measured from the 2D data set. E.COSY (and variants) has found appeal with groups interested in automated analysis of 2D correlation experiments.[3] Surprisingly, there are few or no cases where the E.COSY data have been analysed manually and have thereby effected a full assignment of the ^1H NMR spectrum of a molecule.[4] We wish to show that this may, indeed, be done and have chosen the E.COSY 2D experiment for (+)-glaucine hydrotrifluoroacetate (**1**·HTFA) as an exemplar.

(+)-Glaucine, (6a*S*)-5,6,6a,7-tetrahydro-1,2,9,10-tetramethoxy-6-methyl-4*H*-dibenzo[*de*,*g*]quinoline, (**1**), is an aporphine alkaloid found in *Glaucium flavum*, *Fumariaceae*, *Papveraceae* and in *Dicentra* and *Corydalis* species.[5] It is a non-narcotic antitussive drug.[5]

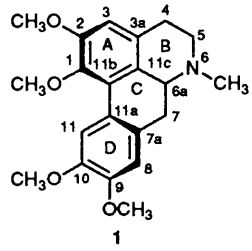

1

The relative configuration of (+)-glaucine was chemically correlated with that for (−)-α-phenylethylamine and for (L)-alanine,[6] and thus the absolute configuration of chirotopic[7] and stereogenic[7] C(6a) is assigned as 6a*S*. The chirotopic and labile stereogenic nitrogen affords two *N*-methyl free base diastereomers which are expected to be at the fast exchange limit (FEL) on the NMR time-scale for interconversion due to facile nitrogen inversion at ambient temperatures. Salts of *N*-substituted azacycles such as (+)-glaucine are also expected to show this diastereomerization phenomenon *via* a prototropic shift/nitrogen inversion mechanism. Dissolution of protonated **1** in chlorinated solvents (such as CD_2Cl_2) should provide the (6*S*,6a*S*)- and (6*R*,6a*S*)-*N*-methyl diastereoisomers (**2** and **3**, respectively) at the kinetic slow exchange rate (SEL) for interconversion. This SEL phenomenon is general and has been demonstrated before (*e.g.* salts of simple piperidines,[8] tropane alkaloids,[9–11] cocaine,[10] morphine,[12–16] nefopam,[17–19] pyrroloisoquinolines,[20–22] *etc.*).

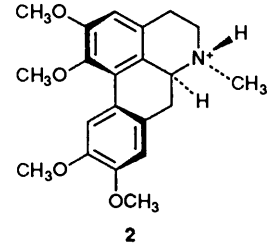

2

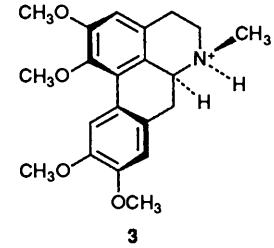

3

In addition, the B-ring within the substituted isoquinoline moiety of **1** is, in principle, capable of partial ring-inversion. The configuration of the stereogenic atoms remain invariant in this process, but the axial/equatorial orientations of ring substituents are interchanged. An excellent example of this is the recent work of Maryanoff *et al.*[20–22] on pyrroloisoquinoline antidepressants (*e.g.* **4**) illustrating solution state interconversion between one *trans* and two *cis* B–C ring-fused isomers. It was thus of interest to study the stereochemistry of (+)-glaucine in solution. The NMR strategy and results of these investigations are presented here.

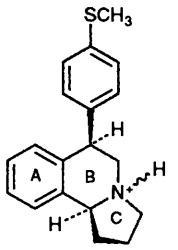

4

Results and Discussion

The 600 MHz ^{1}H NMR spectrum of (+)-glaucine free base has been studied and diastereotopic alicyclic proton assignments were made on the basis of vicinal coupling constant analysis as well as COSY and heterocorrelation (XHCORR) 2D data.[23] Coupling constant data relating to the relative orientation of the B,C-rings was not available since the B-ring 4-spin system is isolated from the C-ring 3-spin system in the free base. In addition, the four reported B-ring vicinal coupling constants for the free base did not unequivocally ascertain the conformation of that ring (see below). However, at slow exchange between the two *N*-methyl diastereomers of the amine salt, vicinal coupling constants involving the N-H proton provide a link between the two spin systems. This provided the impetus to devise an overall strategy based on these extra coupling data and difference-NOE experiments to enable the conformational determination of each diastereomer. A 3:1 ratio of *N*-methyl diastereomers was observed at slow exchange in the ^{1}H NMR spectrum (CD_2Cl_2 solution, 300 K) of (+)-glaucine hydrotrifluoroacetate (**1**·HTFA). Unfortunately, this alkaloid salt afforded a relatively complex ^{1}H NMR spectrum at 300 MHz having a multitude of overlapping peaks and was uninterpretable solely by one-dimensional methods.[24] The **1**·HTFA system can be considered to be more than twice as complicated as that for free base **1** because (*a*) two unequal ratio *N*-methyl diastereomeric species are now present, and (*b*) we were not able to benefit from a spectrometer with such a high static magnetic field. The 3:1 diasteroisomer ratio also mandates that 2D spectra be clean and free of artifacts if assignments for the minor diastereoisomer are to be made with confidence. Since it is not uncommon for a major diastereomeric species cross-peak to be close to that of a minor one, the requisite multiple-quantum filter simplication of the cross-peak pattern must be as close to complete as possible to alleviate potential cross-peak overlap. The E.COSY experiment afforded all proton chemical shift and all the coupling constant data for both *N*-methyl diasteroisomers, and these were then rationalized in terms of solution conformation. Difference-NOE experiments were then used to confirm diastereotopic proton assignments and to finally determine the ring conformations.

The E.COSY experiment has been described in the literature.[2] The single data set was collected, and the data processed using standard methods for phase-sensitive 2D spectra; TPPI in this case. The unsymmetrized data were plotted at an expansion level which permitted the measurement of coupling constants by identification of active and passive couplings. Cross-peaks contain information relating to the mutual scalar coupling (active coupling, *e.g.* $J_{A,X}$ in cross-peak between A and X resonances of an AGMX system) plus coupling involving other nuclei (passive coupling, *e.g.* $J_{A,G}$ and $J_{M,X}$). Thus, cross-peaks in the E.COSY experiment have the same redundancy of information as found in 1D multiplets. We found this to be an asset because it allowed the same coupling constant to be measured several times and averaged. Strong coupling can be a problem in that the (absorptive) cross-peak elements are obscured by the diagonal peaks. Measurement of the relevant

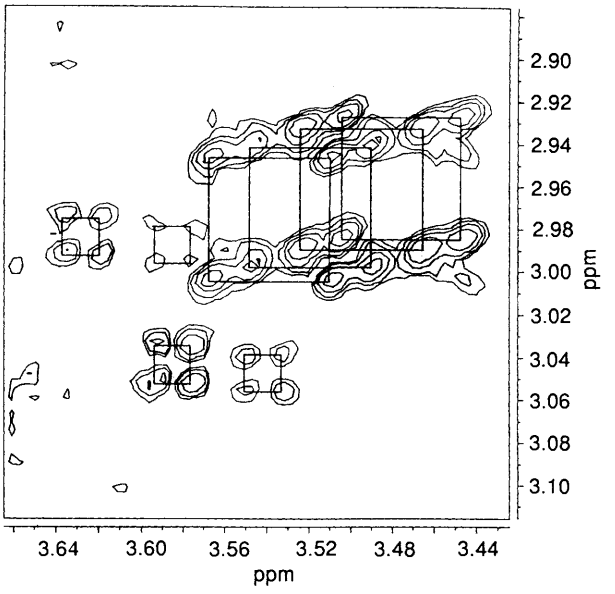

Fig. 1 Expansion of E.COSY 2D NMR spectrum of (+)-glaucine hydrotrifluoroacetate (**1**·HTFA) in CD_2Cl_2 showing the major species H(41,42) cross-peak [negative active coupling constant (−17.9 Hz)] in the upper right-hand corner, and the minor species H(42,51) cross-peak [positive active coupling constant (5.8 Hz)] in the lower left-hand corner.

passive couplings in cross-peaks from another coupled proton may allow one to overcome this problem. Repetition of the active coupling peak pattern within a cross-peak permitted resolution of some cases of cross-peak overlap, since the inherent inversion symmetry in the cross-peak pattern could always be used when part of the total cross-peak was obscured.

It was desired to perform the E.COSY experiment on an N^+–D salt of glaucine as well as on the N^+–H isotopomer so that $^3J_{NH,CH}$ couplings would be absent in the former case. While a preliminary ^{1}H NMR study (300 MHz, CD_2Cl_2) was performed on the HCl salt of **1**,[24] the trifluoroacetate salt of glaucine (**1**·HTFA) was chosen for the E.COSY experiment due to ease of preparing the isotopomeric deuteriotrifluoroacetate salt (**1**·DTFA).

Assignment of the ^{1}H *Nuclei.*—Active coupling was measured from the 'square' repeat pattern of the cross-peak. Two types of repetition of the active coupling 'square' pattern were readily apparent in the E.COSY spectrum. Repetition of the active coupling pattern progressed in a parallel-like direction relative to the diagonal in cross-peaks arising from negative active coupling, while that from positive active coupling progressed in a perpendicular-like manner, see Fig. 1. Cross-peaks arising from geminal and vicinal active couplings were readily differentiated on this basis for both *N*-methyl species. Chemical shifts of actively coupled nuclei were determined from the f1 and f2 projections of the cross-peak inversion centre. Passive couplings to nuclei in the f1 dimension were measured from the displacement of the active coupling pattern in that dimension, while those to nuclei in the f2 dimension were measured by the analogous displacement in f2.

The ^{1}H NMR spectral parameters for the *N*-methyl diastereoisomers of the **1**·HTFA salt are given in Table 1 together with those of the free base[23] **1** from the literature. Parameters measured from the E.COSY spectrum of the **1**·DTFA salt were identical to corresponding values measured from the **1**·HTFA spectrum (with the exception of those involving the N–H nucleus). Inspection of data in Table 1 shows that the coupling constants for the major species of **1**·HTFA are similar to corresponding values for free base **1**. Numerical descriptors for

Table 1 ^{1}H NMR special parameters for (6*S*,6a*S*)/(6*R*,6a*S*) *N*-methyl diastereoisomers of (+)-glaucine hydrotrifluoroacetate (**1**·HTFA) salt *vs.* (+)-glaucine free base (**1**)[a]

	6*S*,6a*S*-Major isomer (**1**·HTFA)	6*R*,6a*S*-Minor isomer (**1**·HTFA)	Free base (**1**)[b]
δ_H			
H(3)	6.67	6.70	—[c]
H(41)	3.51	3.26	3.12
H(42)	2.96	3.01	2.67
H(51)	3.28	3.58	2.45
H(52)	3.85	3.68	3.02
H(6) (N–H)	10.73	11.10	—
N–CH_3	3.16	2.89	2.53
H(6a)	4.01	4.63	3.03
H(71)	3.10	2.95	3.01
H(72)	3.18	3.07	2.57
H(8)	6.80_8	6.81_3[d]	—[c]
H(11)	8.05	8.01	—[c]
C(1)–OCH_3	3.66	3.72	—[c]
3 × OCH_3[e]	3.88, 3.88, 3.86_8	3.89, 3.87, 3.86	—[c]
$J_{H,H}$/Hz			
41, 42	−17.1(2)	−17.9(4)	16.4
41, 51	13.1(3)	12.7(2)	12.6
41, 52	5.5(3)	6.7(3)	6.3
42, 51	4.3(2)	5.2(4)	3.2
42, 52	1.5(2)	1.4(6)	0.6
51, 52	−11.5(1)	−13.1(3)	12.6
6, 51	8.8(5)	<1	—
6, 52	3.3(8)	<1	—
6, 6a	8.5(2)	2.6(4)	—
6, CH_3	5.0(1)[f]	5.1(1)	—
6a, 71	13.2(2)	14.0(1)	13.9
6a, 72	4.8(2)	5.2(3)	3.8
71, 72	−13.4(3)	−12.9(2)	13.9

[a] ppm downfield from tetramethylsilane, 300 MHz, CD_2Cl_2, 298 K, data determined from appropriate E.COSY cross-peak, major:minor ratio *ca.* 3:1, estimated standard deviation (esd) for last digit of *J*-value in parentheses. [b] $CDCl_3$, free base data from ref. 23. [c] Not given. [d] Shoulder. [e] Not assigned. [f] Value was determined from spectrum of the corresponding HCl salt due to overlap in that of the HTFA salt.

nuclei are similar to that used for X-ray crystallography, *e.g.* H(41) and H(42) are both ligated to C(4). For each *N*-methyl species, two types of alicyclic-proton connectivity networks were observed in the E.COSY spectrum of **1**·DTFA in CD_2Cl_2: a 3-spin system consisting of one pair of geminal nuclei [H(71,72)] and one vicinal neighbour [H(6a)], and a 4-spin system consisting of two pairs of adjacent geminal nuclei [H(41,42) and H(51,52)]. Preliminary assignment of major- and minor-species descriptors to each set was made on the basis of cross-peak intensities. Confirmation of major-species descriptor assignment to the appropriate protons was obtained by the observation of nuclear Overhauser effect (NOE) {δ 4.01 [H(6a)]} intensity enhancements of 1.6% and 1.1% to the δ 3.28 [H(51)] and δ 3.02 [N–CH_3] resonances, respectively. The major-species H(41,42) pair was differentiated from the H(51,52) pair by the observation of additional $^3J_{NH,CH}$ coupling for the latter in the E.COSY spectrum of **1**·HTFA. Differentiation for the minor-species pairs was made on the basis of an XHCORR 2D correlation of δ 3.01 [H(42)] with δ 21.95 [C(4)], since $^3J_{NH,CH}$ coupling was not measured for minor species H(51,52). Aromatic H(3,8,11) protons were assigned by analogy to the relative magnitudes of literature values[25] for free base **1**. Values of 8.3, 8.0 and 3.5 Hz were estimated for major species $J_{6,51}$, $J_{6,6a}$, and minor species $J_{6,6a}$, respectively, upon homonuclear decoupling of the appropriate N–H proton. Inspection of these values with those in Table 1 show that they compare quite reasonably with those measured from the E.COSY spectrum.

^{13}C *NMR Details.*—Extensive ^{13}C NMR studies of aporphine alkaloid free bases has been performed by Jackman, Wenkert and co-workers[26] and also by Ricca and Casagrande.[27] The latter authors also reported the results for one aporphine salt in [$^2H_6$]DMSO, but no mention was made of the appearance of more than one solution species.[27] The ^{13}C NMR spectral parameters for the *N*-methyl diastereomers of **1**·HTFA salt are given in Table 2 together with those of the free base **1**.[26,27] Inspection of data in Table 2 shows that chemical shifts for the major species of **1**·HTFA are similar to corresponding values for carbons in free base **1**. Multiplicities of resonances in the ^{13}C {^{1}H} NMR spectrum were determined by comparison with DEPT spectra (90° and 135° pulse widths). Assignments of protonated carbons were made from a ^{13}C/^{1}H 2D-NMR heterocorrelation spectrum ($^1J_{C,H}$), while quaternary ^{13}C nuclei chemical shifts were assigned by analogy to the relative magnitudes of literature vales[26] for free base **1**.

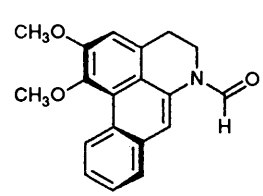

5

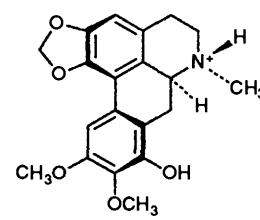

6

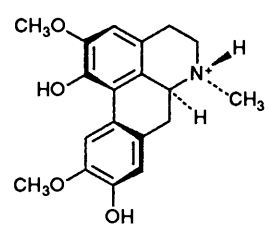

7

Stereochemistry.—The biphenyl moiety present in aporphine alkaloids is usually twisted. Torsion angle C(7a)–C(11a)–C(11b)–C(11c) is *ca.* +20° in solid-state structures of 6a*S*-aporphines, and as such these may be assigned a (11a,11b-a*R*) CIP[28] chirality descriptor. The twist decreases in magnitude in trigonal-C(6a) dehydroaporphine alkaloids [*e.g. ca.* 5° in crystalline *N*-desmethyl-*N*-formyldehydronuciferine[29] (**5**)]. Due to the fused B- and C-rings, the chirality of the twisted biphenyl is not an independent stereogenic element in the tetragonal-C(6a) aporphine skeleton,[30–33] *e.g.* X-ray crystallographic structure determination has shown that the 6a*S*-chirality of leucoxinium[33] (**6**) and isoboldinium cations[33] (**7**) is linked with (11a,11b-a*R*) axial chirality.

The skew or twist of the aporphine B-ring represents another stereogenic element, *e.g.* *P*-type or *M*-type conformations [descriptor is based on the sign of torsion angle C(3a)–C(4)–C(5)–N, see Table 3]. The above *M*-conformation for the cyclohexenyl B-ring of the isoquinoline moiety is a well-behaved 'flattened-chair' type since (*a*) there are alternating signs for the ring torsion angles, (*b*) the magnitudes of ∠C(3a)–C(4)–C(5)–N, ∠C(4)–C(5)–N–C(6a), and ∠C(5)–N–C(6a)–C(11c) are reasonably similar to those in a chair (*e.g.* −42°, 64°, −51°, respectively, for the B-ring of crystalline **7**), and (*c*) protons on C(6a) and C(4) have a *trans*-1,4-diaxial relationship. The *P*-conformation is only a pseudo 'flattened-chair' type since while ∠C(3a)–C(4)–C(5)–N, ∠C(4)–C(5)–N–C(6a), and ∠C(5)–N–C(6a)–C(11c) remain reasonably similar to those in a chair (*e.g.* 64°, −64°, 27°, respectively, for the B-ring of crystalline **8**), ∠N–C(6a)–C(11c)–C(3a) does not have the proper sign (presumably due to fusion of the B,C-rings). A search of the

Table 2 ^{13}C NMR spectral parameters for (6*S*,6a*S*)/(6*R*,6a*S*)-*N*-methyl diastereoisomers of (+)-glaucine hydrotrifluoroacetate salt (**1**·HFTA) *vs.* (+)-glaucine free base (**1**)[a]

	1·HFTA		**1**	
δ_C(ppm)	6*S*,6a*S*-*major*	6*R*,6a*S*-minor	lit. ref. 26[b]	lit. ref. 27[c]
C(1)	145.60		144.2	143.7
C(2)	154.09		151.8	151.5
C(3)	110.81	110.92	110.4	110.9
C(3a)	126.65[d]		128.8	126.9
C(4)	26.36	22.06	29.2	28.8
C(5)	54.09	51.12	53.3	52.6
N-CH_3	42.80	33.71	43.4	43.6
C(6a)	63.98	59.61	62.5	62.1
C(7)	32.06	31.46	34.5	33.8
C(7a)	127.46		129.3	129.4
C(8)	111.62	111.62	110.9	111.0
C(9)	149.21		148.0	147.9
C(10)	148.61		147.4	146.1
C(11)	112.52	112.52	111.6	111.6
C(11a)	120.66		124.4	123.7
C(11b)	124.05		126.8	125.9
C(11c)	126.29[d]		127.2	
C(1)-OCH_3	60.34	60.51	60.0	59.4
OCH_3[e]	56.34, 56.06, 56.06	56.17, 56.17, 56.17	55.6, 55.7, 55.8	55.5, 55.5, 55.3

[a] ppm downfield from tetramethylsilane, 75 MHz, CD_2Cl_2, 298 K, major:minor ratio *ca.* 3:1. [b] $CDCl_3$. [c] [$^2H_6$]DMSO. [d] Assignments may be reversed. [e] Not assigned.

Table 3 Selected torsional angles for the molecular mechanics calculated models **15**–**18** of (+)-glaucine cation *vs.* (6a*S*)-isoboldine·HBr (**7**) and (6a*S*)-*N*-acetyl-1-(*O*-acetyl)-laurelliptine (**8**)

Torsion angle	**15** (6*S*,6a*S*,*M*)	**16** (6*R*,6a*S*,*M*)	**17** (6*S*,6a*S*,*P*)	**18** (6*R*,6a*S*,*P*)	**7** (6*S*,6a*S*,*M*)[a]	**8** (6a*S*,*P*)[b]
C(6a)-C(11c)-C(3a)-C(4)	−2	0	−3	−6	0	−3
C(11c)-C(3a)-C(4)-C(5)	21	16	−36	−28	10	−33
C(3a)-C(4)-C(5)-N	−52	−48	60	61	−42	64
C(4)-C(5)-N-C(6a)	68	64	−45	−64	64	−64
C(5)-N-C(6a)-C(11c)	−48	−47	5	30	−51	27
N-C(6a)-C(11c)-C(3a)	15	16	20	5	21	8
C(7a)-C(11a)-C(11b)-C(11c)	21	19	19	20	21	24
C(11a)-C(11b)-C(11c)-C(6a)	2	1	2	5	−1	3
C(11b)-C(11c)-C(6a)-C(7)	−41	−38	−39	−44	−38	−45
C(11c)-C(6a)-C(7)-C(7a)	58	55	55	59	56	61
C(6a)-C(7)-C(7a)-C(11a)	−39	−39	−38	38	−40	−37
C(7)-C(7a)-C(11a)-C(11b)	−1	−2	0	−2	1	−6
H(41)-C(4)-C(5)-H(51)	−172	−167	179	180		
H(41)-C(4)-C(5)-H(52)	−54	−50	63	61		
H(42)-C(4)-C(5)-H(51)	−54	−51	60	61		
H(42)-C(4)-C(5)-H(52)	64	66	−56	−58		
H(6)-N-C(5)-H(51)	−170	58	−38	172		
H(6)-N-C(5)-H(52)	71	−57	77	−69		
H(6)-N-C(6a)-H(6a)	−174	−45	−120	31		
H(6a)-C(6a)-C(7)-H(71)	−179	−178	−179	−175		
H(6a)-C(6a)-C(7)-H(72)	62	63	63	66		
Relative energy (kJ mol^{-1})	0.00	1.21	0.92	6.40		

[a] Calculated from X-ray coordintes in ref. 33. [b] Calculated from X-ray coordinates in ref. 34.

crystallographic literature shows both B-ring chair conformations for the 6a*S*-family of aporphines. Both crystalline sp^2-*N* alkaloids (6a*S*)-*N*-acetyl-1-(*O*-acetyl)-laurelliptine[34] (**8**) and (6a*S*)-*N*,*O*-diacetyl-4-hydroxynornantenine[35] (**9**) exhibit B-ring *P*-chair conformations. While substitution of the C(4) *pro-R* hydrogen enables the 4*R*-acetyloxy substituent to reside in an equatorial disposition on the B-ring *P*-chair of **9**, this does not appear to be a necessary requisite since the unsubstituted B-ring of **8** also shows the same solid-state conformational preference (see Fig. 2). On the other hand, sp^3-*N* crystalline 6a*S*-laurelliptine[36] free base (**10**) has a B-ring *M*-chair. In general, crystalline sp^3-N 6a*S*-aporphine salts [*e.g.* leucoxine·HBr[33] (**6**), isoboldine·HBr[33] (**7**), apomorphine·HCl[37] (**11**), bulbocapnine·MeI (**12**)[38]] seem to show a propensity for B-ring *M*-chair conformations in the solid-state, see Fig. 2.

Maryanoff *et al.*[20] have shown solution-state interconversion between *cis*-(4*S*,10b*R*,*M*)-, *cis*-(4*S*,10b*R*,*P*)-, and *trans*-(4*R*,-10b*R*,*M*)-1,2,3,5,6,10b-hexahydropyrrolo[2,1-*a*]isoquinoline·HBr diastereomeric salts upon dissolution of the latter solid isomer in chloroform. ^1H NMR spectroscopy revealed that protonated *cis*-compounds readily underwent ring-inversion thereby interconverting the *M* and *P* B-ring chair-conformations **13** and **14** (see Fig. 2), while *cis*–*trans* interconversions occurred *via* a prototropic shift/nitrogen inversion.[20–22]

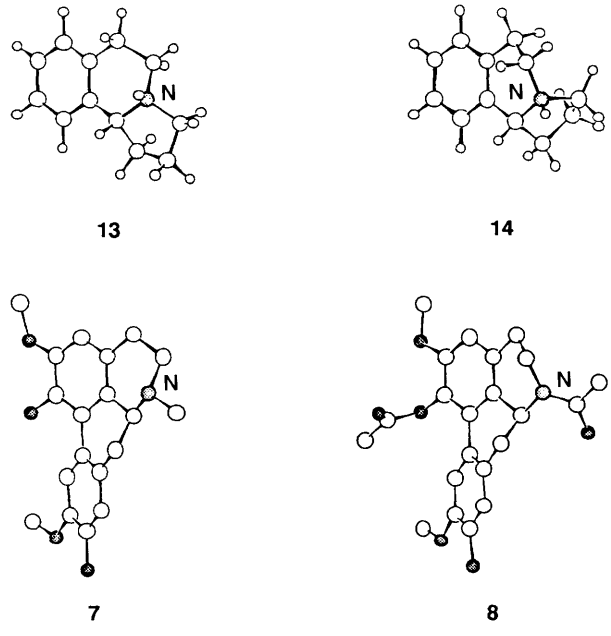

Fig. 2 X-Ray crystallographically determined molecular structures of sp^3-N (6a*S*,*M*)-isoboldine·HBr [33] (**7**) and sp^2-N (6a*S*,*P*)-*N*-acetyl-1-(*O*-acetyl)laurelliptine [34] (**8**), and molecular mechanics determined structures of (4*S*,10b*R*,*M*)- and (4*S*,10b*R*,*P*)-*cis*-1,2,3,5,6,10b-hexahydropyrrolo[2,1-*a*]isoquinolinium cations (**13** and **14**, respectively), illustrating the *M*- and *P*- B-ring chair-type conformations.

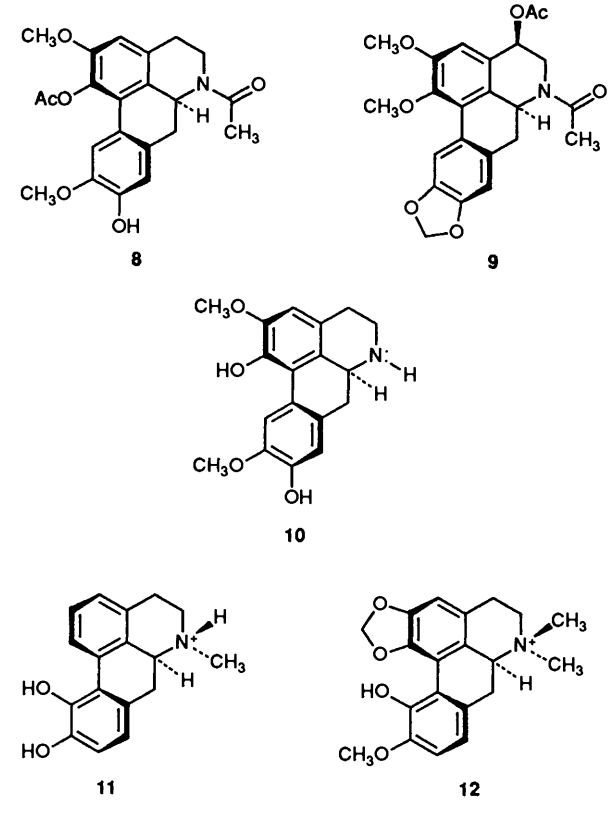

Molecular mechanics models were calculated for four 6a*S*-aporphine diastereomeric structures [(6*S*,6a*S*,*M*)-**15**, (6*R*,6a*S*,*M*)-**16**, (6*S*,6a*S*,*P*)-**17** and (6*R*,6a*S*,*P*)-**18**] using the MMX89 [39] program in order to determine the structure of the major and minor (+)-glaucine solution-state species. MMX89 is an enhanced version of Allinger's MM2 program [40a] with MMP1 π-subroutines [40b] incorporated for localized π-electron systems. Torsion angles *H*–C–C–*H* for vicinal alicyclic protons are listed in Table 3 for each model. Models **16**, **17** and **18** were calculated

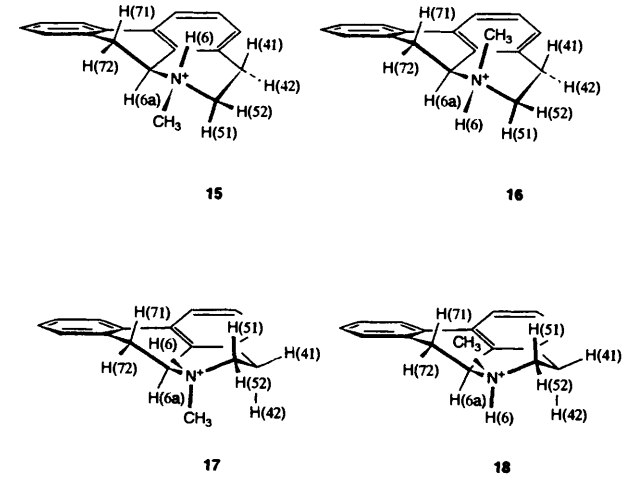

to have 1.21, 0.92 and 6.40 kJ mol^{-1} higher energy, respectively, than **15**. Note, there are two equatorial *N*-methyl diastereoisomers [(6*S*,6a*S*,*M*)-**15** and (6*R*,6a*S*,*P*)-**18**] and two axial *N*-methyl diastereoisomers [(6*R*,6a*S*,*M*)-**16** and (6*S*, 6a*S*,*P*)-**17**].

Two B-ring conformations (**I** and **II**) for free base **1** were discussed by Kerr *et al.*,[23] although they were not adequately characterized. Nor was the interconversion process described. Conformation **I** in their work [23] appears pictorially similar to that for model **15** with an equatorial *N*-methyl, while conformation **II** looks like a ring-inverted half-chair with an axial *N*-methyl. Molecular mechanics modelling shows that their half-chair conformation **II** does not represent an energy minimum, but it is very similar to model **17**. The authors concluded that conformation **I** was preponderant in solution for the free base **1**, since they observed a large (12.6 Hz) coupling constant for two vicinal diaxial protons in the C(4)–C(5) dimethylene fragment.[23] The difficulty is that the C(4)–C(5) dimethylene fragment has an antiperiplanar torsion angle H(41)–C(4)–C(5)–H(51) in each of the four models (**15**–**18**), see Table 3. In *M*-conformation B-rings (models **15**, **16**), the *pro-R* protons on C(4,5) are diaxial, while in *P*-conformation B-rings (models **17**, **18**), these are the *pro-S* protons. Therefore, one cannot unequivocally ascertain the B-ring conformation solely from vicinal coupling constants involving the C(4)–C(5) fragment alone.

In both solution species, each of the diastereotopic H(71,72) protons have a different relationship to H(6a) [*i.e.* a large antiperiplanar magnitude $J_{6a,71}$ value and a smaller synclinal (gauche) magnitude $J_{6a,72}$ value for each species]. The appearance of one antiperiplanar and three synclinal magnitude vicinal coupling constants for the C(4)–C(5) fragment in both major and minor species is consistent with a gauche conformation for –C(3a)–C(4)–C(5)–N–. Since all four $^3J_{H,H}$ values are known for this fragment in both the major and minor species, dihedral angle C(3a)–C(4)–C(5)–N can be calculated for both solution species using the R-factor method [41] of Lambert. Orientation and electronegativity effects of X,Y-substituents in the $-X-CH_2-CH_2-Y-$ fragment are cancelled out in this ratio method.[41] These values are calculated to be 53° (major species) and 48° (minor species). H(6) (N–H) has markedly unequal magnitude vicinal coupling constants involving the two diastereotopic H(51,52) neighbours in the major species [8.8(5) and 3.3(8) Hz for $J_{6,51}$ and $J_{6,52}$, respectively]. This suggests two different orientations for diastereotopic H(51,52) relative to N–H [*i.e.* H(51) and H(52) are respectively disposed in an antiperiplanar and synclinal manner *vis-a-vis* N–H]. In addition, since the magnitudes of $J_{6,51}$ and $J_{6,6a}$ are similar, we expect H(6a) to also be antiperiplanar to N–H, and the *N*-methyl group must be equatorial in the major species. Of

the two models with equatorially orientated *N*-methyl groups, the H–C–C–H torsion angles of model **15** are more consistent with the observed vicinal coupling constants than are those of model **18**.

Nuclear Overhauser effect experiments readily differentiated between these two equatorial *N*-methyl candidates for the major species, and showed that the lowest calculated energy structure of the four models (6*S*,6a*S*,*M*-model **15**) is the major solution-state species. A 2.4% and 2.9% intensity enhancement was observed for major species H(6a) and H(42), respectively, upon {δ 3.28 [H(51)]}, and a 1.6% and 1.1% NOE was found for major species H(51) and N–CH_3, respectively, upon {δ 4.01 [H(6a)]}. Nuclei H(51) and H(6a) are in a *cis* 1,3-diaxial arrangement in model **15** [2.504 Å, internuclear distance], while in model **18** they are on opposite sides of the B-ring.

The 2.6(4) Hz value of $J_{6.6a}$ for the minor species is consistent with an axial orientation for the *N*-methyl group in the minor solution-state species. Of the two axially orientated *N*-methyl models, the H–C–C–H torsion angles of model **16** are more consistent with the observed vicinal coupling constants than are those of model **17**. Again, the NOE experiment easily differentiates between the two axial *N*-methyl candidates for the minor species. A 4.0% NOE was observed for minor species H(71) upon {δ 2.89 [N–CH_3]}. The methyl group and the H(71) nucleus have a *cis* 1,3-diaxial relationship in model **16**, while in model **17** they are located on opposite sides of the molecule. Thus, this result confirms 6*R*,6a*S*,*M*-model **16** as the minor solution-state species which arises from **15** *via* a prototropic shift/nitrogen inversion mechanism. The 3:1 major:minor ratio is in accord with the small energy difference calculated for models **15** and **16**. The solution-state ∠C(3a)–C(4)–C(5)–N values of 53° (major species) and 48° (minor species) are in very good agreement with the 52° and 48° values for the two respective B-ring *M*-conformations in the molecular mechanics calculated models (as opposed to the larger 60–61° values for the *P*-conformations).

The relative change in ^{13}C NMR chemical shifts of externally diastereotopic nuclei in the two *N*-methyl epimers are also in agreement with an assignment of an equatorial *N*-methyl group in the major species and an axial one in the minor solution species. Carbons β to the methyl are shifted upfield in the axial *N*-methyl minor species [C(5) and C(6a) by 2.97 and 4.37 ppm, respectively]. There is a shift of 9.04 ppm upfield for the axial methyl carbon (relative to the equatorial one), while C(4) in the γ-position is shifted 4.31 ppm upfield (the so-called 'γ-effect').[42] A similar *ca.* 10 ppm chemical shift difference has also been noted for internally diastereotopic methyl carbons in aporphine·MeI[26] quaternary ammonium salts.

The large chemical shift difference between externally diastereotopic *N*-methyl carbons at the SEL for isomer interconversion is also observed for free bases (at appropriately low temperatures), *e.g.* $\Delta\delta$ 8.49 ppm for tropine free base[43] [δ 41.13 (eq.) and 32.64 (ax.) at −70 °C in $CFCl_3$/MeOH, $\Delta G^{\ddagger}_{233}$ = 46.4 kJ mol^{-1}; (δ 40.3 FEL in $CDCl_3$)[44]], and is usually about an order of magnitude higher than the $\Delta\delta$ due to protonation of the free base, *e.g.* atropine free base[44] FEL δ 40.24 in $CDCl_3$ and atropine methane sulphonic acid salt *N*-methyl diastereoisomers[10] [δ 39.27 (eq.) and 31.95 (ax.) SEL in CD_2Cl_2]. Since the FEL chemical shift of *ca.* 43.5 ppm[26,27] reported for glaucine free base **1** is very close to the SEL 42.80 ppm value for the equatorial *N*-methyl salt, and is quite different from 33.71 ppm for the axial *N*-methyl, this suggests that the equatorial *N*-methyl orientation is likely to be the major contributor to the free base time-averaged FEL structure. A 51° dihedral ∠C(3a)–C(4)–C(5)–N was found using the $^3J_{H.H}$ coupling constants for the C(4)–C(5) fragment reported by Kerr *et al.*[23] Of the two candidates with equatorial *N*-methyl groups, the calculated free base 6*S*,6a*S*,*M*-model has a value of 50°, while it is slightly larger (54°) for the ring and nitrogen inverted 6*R*,6a*S*,*P*-model. As with the protonated cation **1**·HTFA, the 6*S*,6a*S*,*M*-model for **1** is also the minimum energy structure of the four calculated in the free base series. While the $^3J_{H.H}$ coupling constants, ^{13}C NMR data, and molecular mechanics modelling are all consistent with the major contributor to the free base FEL structure **1** having a structure similar to that of the 6*S*,6a*S*,*M*-equatorial *N*-methyl diastereoisomer **1**·HTFA, NOE experiments on **1** should be performed to prove this point.

Experimental

(+)-Glaucine was purchased from Aldrich Chemical Co., Inc. The trifluoroacetate/deuteriotrifluoroacetate salt was obtained by treating a CD_2Cl_2 solution of the alkaloid with 1.1 equivalents of the appropriate acid. ^{1}H and ^{13}C NMR spectra (7.05 T, CD_2Cl_2, sealed 5 mm sample tube, 298 K) were obtained at 300.1 and 75.5 MHz, respectively, on a Bruker AM-300 Fourier transform spectrometer equipped with an Aspect 3000 data system. The deuteriated solvent was used as internal lock, and the residue protio solvent was used an internal secondary reference [δ_H 5.32 and δ_C 53.8 relative to tetramethylsilane]. Standard Bruker microprograms were used for the DEPT (90° and 135° pulse angles), difference-NOE (NOEDIFF), and XHCORR experiments. The E.COSY experiment was performed using the Bruker Library microprogram (ECOSY4N) which used TPPI to afford a phase-sensitive acquisition. K_c Values were chosen to select up to four-quantum coherence. The digital resolution was 1.6 Hz/pt in each dimension after a single zerofill in f1.

The minimized-energy geometry of the molecular mechanics calculated model compounds were determined by the MMX89 program,[40] and were performed on a Micro VAX-II computer under Micro VMS V4.5.

Acknowledgements

Gratitude is expressed by R. G. for hospitality extended to him by the Merck Frosst Centre for Therapeutic Research. Thanks are also given to Ms. Rosita Rostiker (Ben-Gurion University), Prof. Arthur S. Perlin (McGill University) and Dr. Qin-Ji Peng (McGill University/Dalian University) for preliminary assistance and discussions.

References

1 M. A. Bernstein, in *Two-Dimensional NMR Spectrocopy*, eds. W. R. Croasmun and R. M. K. Carlson, VCH, New York, 1987, pp. 233–257.
2 (*a*) C. Griesinger, O. W. Sørensen and R. R. Ernst, *J. Am. Chem. Soc.*, 1985, **107**, 6394; (*b*) *J. Chem. Phys.*, 1986, **85**, 6837; (*c*) *J. Magn. Reson.*, 1987, **75**, 474.
3 Z. Mádi, B. U. Meier and R. R. Ernst, *J. Magn. Reson.*, 1987, **72**, 584.
4 H. Kessler, J. W. Bats, C. Griesinger, S. Koll, M. Will and K. Wagner, *J. Am. Chem. Soc.*, 1988, **110**, 1033.
5 *Merck Index*, ed. S. Budavari, 11th edn., Rahway NJ, 1989, p. 695 and references therein.
6 H. Corrodi and E. Hardegger, *Helv. Chim. Acta*, 1956, **39**, 889.
7 K. Mislow and J. Siegel, *J. Am. Chem. Soc.*, 1984, **106**, 3319.
8 A. F. Casy, *PMR Spectroscopy in Medicinal and Biological Chemistry*, Academic Press, London, 1971, Chapter 4.
9 G. L. Closs, *J. Am. Chem. Soc.*, 1959, **81**, 5456.
10 R. Glaser, Q.-J. Peng and A. S. Perlin, *J. Org. Chem.*, 1988, **53**, 2172.
11 K. H. Pook, W. Schulz and R. Banholzer, *Justus Liebigs. Ann. Chem.*, 1975, 1499.
12 J. Glasel, *Biochem. Biophys. Res. Commun.*, 1981, **102**, 703.
13 C. E. Brown, S. C. Roerig, J. M. Fujimoto and V. T. Burger, *J. Chem. Soc., Chem. Commun.*, 1983, 1506.
14 E. L. Elliel, S. Morris-Natschke and V. M. Kolb, *Org. Magn. Reson.*, 1984, **22**, 258.

15 J. Glasel and H. W. Reiher, *Magn. Reson. Chem.*, 1985, **23**, 236.
16 J. Glasel and P. N. Borer. *Biochem. Biophys. Res. Commun.*, 1986, **141**, 1267.
17 R. Glaser. S. Cohen. D. Donnell and I. Agranat, *J. Pharm. Sci.*, 1986, **75**. 772.
18 R. Glaser, G. Frenking. G. H. Loew, D. Donnell and I. Agranat, *New J. Chem.*, 1988, **12**, 953.
19 R. Glaser, *Magn. Reson. Chem.*. 1986, **75**, 772.
20 B. E. Maryanoff. D. F. McComsey, J. F. Gardocki, R. P. Shank, M. J. Costanzo, S. O. Nortey. C. R. Schneider and P. E. Setler, *J. Med. Chem.*, 1987. **30**, 1433.
21 B. E. Maryanoff, D. F. McComsey, R. R. Inners. N. S. Mutter, G. P. Wooden. S. L. Mayo and R. A. Olofson, *J. Am. Chem. Soc.*, 1989, **111**. 2487.
22 K. L. Sorgi, C. A. Maryanoff, D. F. McComsey, D. W. Graden and B. E. Maryanoff, *J. Am. Chem. Soc.*, 1990, **112**, 3567.
23 K. M. Kerr. A. M. Kook and P. J. Davis, *J. Nat. Prod.*, 1986, **49**, 576.
24 R. Glaser, Q.-J. Peng and A. S. Perlin, unpublished results.
25 A. H. Jackson and J. A. Martin, *J. Chem. Soc. C*, 1966, 2061.
26 L. M. Jackman. J. C. Trewella, J. L. Moniot, M. Shamma, R. L. Stephens, E. Wenkert, M. Leboeuf and A. Cavé, *J. Nat. Prod.*, 1979, **42**. 437.
27 G. S. Ricca and C. Casagrande, *Gazz. Chim. Ital.*, 1979, **109**, 1.
28 R. S. Cahn. C. Ingold and V. Prelog, *Angew. Chem., Int. Ed. Engl.*, 1966. **5**. 385.
29 T. Nozaka, I. Morimoto, M. Ishino, T. Okitsu, H. Kondoh, K. Kyogoku. Y. Sugawara and H. Iwasaki. *Chem. Pharm. Bull.*, 1987, **35**, 2844.
30 S. Goodwin. J. N. Shoolery and L. F. Johnson, *Proc. Chem. Soc.*, 1958, 306.
31 (*a*) M. Shamma, *Experientia*, 1960, **16**, 48; (*b*) *Experientia*, 1962, **18**, 64.
32 C. Djerassi, K. Mislow and M. Shamma, *Experientia*, 1962, **18**, 53.
33 G. M. Brown and L. H. Hall, *Acta Crystallogr., Sect. B*, 1977, **33**, 2051.
34 R. Roques, J. P. Declercq and G. Germain, *Acta Crystallogr., Sect. B*, 1978, **34**, 2017.
35 V. Zabel, W. H. Watson, A. Urzua and B. K. Cassels, *Acta Crystallogr., Sect. B*, 1979, **35**, 3126.
36 R. Roques, L. A. Djakoure and J. C. Rossi, *Acta Crystallogr., Sect. B*, 1978, **34**, 837.
37 J. Giesecke, *Acta Crystallogr., Sect. B*, 1973, **29**, 1785.
38 C. H. Wei, S. P. Basu, J. R. Einstein and B. E. Hingerty, *Acta Crystallogr., Sect. C*, 1984, **40**, 1737.
39 MMX89, Serena Software Inc., Bloomington, Indiana.
40 (*a*) N. L. Allinger, *J. Am. Chem. Soc.*, 1977, **99**, 8127; (*b*) N. L. Allinger and J. L. Sprague, *J. Am. Chem. Soc.*, 1973, **95**, 3893.
41 (*a*) J. B. Lambert, *J. Am. Chem. Soc.*, 1967, **89**, 1836; (*b*) J. B. Lambert, *Acc. Chem. Res.*, 1971, **4**, 87.
42 D. K. Dalling and D. M. Grant. *J. Am. Chem. Soc.*, 1974, **96**, 1827 and references therein.
43 H. J. Schneider and L. Stürm, *Angew. Chem., Int. Ed. Engl.*, 1976, **15**, 545.
44 P. Hanisch, A. J. Jones, A. F. Casy and J. E. Coates, *J. Chem. Soc., Perkin Trans. 2*, 1977, 1202 and references therein.

Paper 1/03229A
Received 28*th June* 1991
Accepted 18*th August* 1991